Laboratori Nazionali di Frascati

LNF-92/026 (P)
9 Aprile 1992

ENSLAPP-A-376/92

J.L. Franzini, W. Kim, P.J. Franzini

BACKGROUNDS AND INTERFERENCE ON THE f_0

Contribution to the DAΦNE Physics Handbook

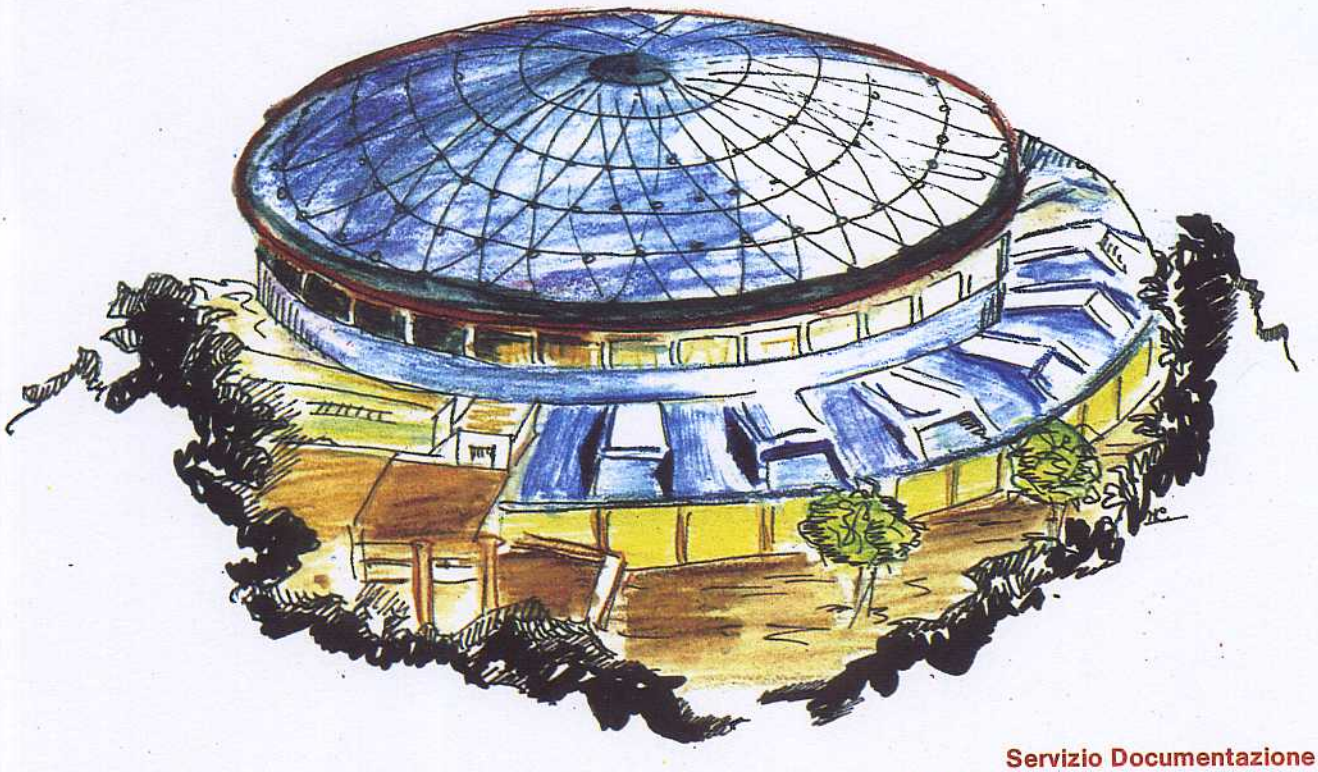

Servizio Documentazione
dei Laboratori Nazionali di Frascati
P.O. Box, 13 - 00044 Frascati (Italy)

LNF-92/026 (P)
9 Aprile 1992

ENSLAPP-A-376/92

J.L. Franzini, W. Kim, P.J. Franzini

BACKGROUNDS AND INTERFERENCE ON THE f_0

Contribution to the DAΦNE Physics Handbook

INFN - Laboratori Nazionali di Frascati
Servizio Documentazione

LNF-92/026 (P)
9 Aprile 1992

ENSLAPP-A-376/92

BACKGROUNDS AND INTERFERENCE ON THE f_0

JULIET LEE-FRANZINI

Laboratori Nazionali di Frascati dell'INFN

SUNY at Stony Brook, Stony Brook, New York 11794

WON KIM

SUNY at Stony Brook, Stony Brook, New York 11794

PAULA J. FRANZINI

Laboratoire D'Annecy-Le-Vieux de Physique des Particules, Annecy, France

ABSTRACT

We present in this paper a complete study of the physical backgrounds, coherent and incoherent, in the 20-100 MeV photon spectrum from $e^+e^- \to \pi^+\pi^-\gamma$ at the ϕ peak, of relevance to $\phi \to f_0\gamma \to \pi^+\pi^-\gamma$. Continuum contributions are suppressed by suitable kinematics and angular cuts. We show that we can determine the sign of the $\phi f_0\gamma$ coupling even for the smallest branching ratio expected for $\phi \to f_0\gamma$, thus have the promise of a totally new piece of information on the nature of the f_0.

1. INTRODUCTION

In a previous paper we have studied measuring the branching ratio, BR, for $\phi \to f_0\gamma$ using both the $f_0 \to \pi^0\pi^0$ (neutral) decay channel and the $f_0 \to \pi^+\pi^-$ (charged) decay channel.[1] We had considered in detail the backgrounds which arise from other decay channels of the ϕ. They constitute the only backgrounds for the neutral decays, and we have demonstrated that, for this case, the $\phi \to f_0\gamma$ BR is easily measured at DAΦNE with a minimal, precision, calorimeter such as CUSB, and can be superbly done with KLOE. However, in the charged channel, additional backgrounds come from continuum processes such as coupling of the initial e^+e^- state to the tail of the ρ, an *initial state radiation process*, and $e^+e^- \to \mu^+\mu^-\gamma$ if mûons are mistaken for pions. Furthermore, the ϕ can produce a pair of pions through off-shell ρ production with one of the pions radiating a γ, a *final state radiation process*. We shall call A_{ρ^*} the amplitude for this process and A_{f_0} the amplitude for $\phi \to f_0\gamma \to \pi^+\pi^-\gamma$.

A_{ρ^*} and A_{f_0} must be added because the pions from ρ decay with final state radiation are in a C-even state, as are those from f_0 decay.[2] The sign of the interference term is unknown, since it depends on the sign of the $\phi f_0\gamma$ coupling and therefore on the unknown nature of the f_0.[3] While the magnitude of final state radiation is approximately one tenth of that for initial state radiation, the f_0 signal is comparable, or could be orders of magnitude smaller than it. Thus the interference term can drastically alter the f_0 signal in ϕ decays, both in shape and in magnitude. For the case of destructive interference, the f_0 signal can become woefully small. However, since the shape of the interference term and its angular distributions are different from those from $|A_{f_0}|^2$, the presence of an f_0 signal can always be recognized, even when cancellation is maximal. We only lose sensitivity to the presence of f_0's in ϕ decays when BR($\phi \to f_0\gamma$) becomes smaller than 1×10^{-6}. In addition the shape of the signal allows in general to determine the sign of the interference term and therefore of the $\phi \to f_0\gamma$ amplitude, another valuable piece of information about the mysterious f_0. The $\mu^+\mu^-\gamma$ background is easily removed in KLOE (section 2), and the initial state radiation can be strongly suppressed by angular cuts (section 3). Thus we find the conclusions of ref. 2 more pessimistic than necessary.

2. $e^+e^- \to \mu^+\mu^-\gamma$

At the ϕ peak resonance energy, the cross section for $e^+e^- \to \mu^+\mu^-\gamma$ where the photon energy is between 10 and 120 MeV is 4.8 nb, equivalent to a BR of 1×10^{-3}, orders of magnitude larger than the signal from $f_0 \to \pi^+\pi^-\gamma$ where BR is expected to be at the most 1.3×10^{-4}.[4] In the KLOE detector[5] there is no dedicated particle identification system. The large background contribution from $e^+e^- \to \mu^+\mu^-\gamma$ can however be fully controlled in KLOE because of its good momentum resolution.

While the calorimeter resolution at low energies is relatively poor, events with two charged particles and a photon are four times overconstrained. For ϕ production at rest, momentum conservation gives $E_\gamma = |\mathbf{p}^+ + \mathbf{p}^-|$. From energy conservation, assuming that the positive and negative particles are pions, we get $E'_\gamma = M_\phi - E^+ - E^-$. For $\phi \to \pi^+\pi^-\gamma$ we expect $E_\gamma = E'_\gamma$, while for $e^+e^- \to \mu^+\mu^-\gamma$, the two energies differ by about 17.5 MeV, having used the pion mass for the muons. We have generated by Monte Carlo (MC) simulations the difference $\Delta E_\gamma = E_\gamma - E'_\gamma$, using the expected KLOE momentum resolution.[5] For $\phi \to \pi^+\pi^-\gamma$ decays we find that the rms spread of ΔE_γ is 2 MeV and for $e^+e^- \to \mu^+\mu^-\gamma$, ΔE_γ=17.5 MeV, also with a spread of 2 MeV. Therefore, a cut at in ΔE_γ at 8 MeV gives us a rejection factor of $\sim$2400 against the muon background, which in fact makes it negligible with respect to any other processes with pions in the final states. Note that we have not used the well measured photon direction (±5 mrad) for additional help.

3. $e^+e^- \to \pi^+\pi^-\gamma$

The f_0 candidates can be first selected by requiring that only a pair of nearly collinear, oppositely charged tracks and one low energy photon, $20 < E_\gamma < 100$ MeV, are present in the detector. We also ask that the visible energy equals W, the total energy. Finally we require that $\Delta E_\gamma < 8$ MeV, in order to eliminate the $\mu^+\mu^-\gamma$ background.

Four amplitudes, A_1, A_2, A_{ρ^*} and A_{f_0} contribute to the $\pi^+\pi^-\gamma$ final state. The corresponding intensities, $|A_1|^2$, $|A_2|^2$ and $|A_{\rho^*}|^2$ are background contributions and the f_0 signal is contained in $|A_{f_0}|^2$ and $2\Re(A_{\rho^*}A^*_{f_0})$, as explained above and discussed below.

3.1 A_1

A_1=$A(\phi\to\pi_1\rho^*\to\pi_1\pi_2\gamma)$. This is the amplitude for $\phi\to\pi^+\pi^-\gamma$ via a $\pi\rho^*$ with the ρ^* coupling to $\gamma\pi$, ρ^* here stands for an internal line, virtual ρ in the corresponding Feynman amplitude. This process, including its angular dependence,[6] has been studied in detail and discussed in our previous paper.[1] Its contribution to the background is small compared to the other sources, see fig. 1a.

3.2 A_2

A_2=$A(e^+e^-\to\gamma\gamma\to\rho^*\gamma\to\pi^+\pi^-\gamma)$. This amplitude from *initial state radiation* is the largest incoherent source of background. However, since, as seen from figure 5a of Ref. 2 $|A_2|^2$ is peaked very sharply at small angles between the photon and the beam, $\theta_{\gamma,\ \mathrm{beam}}$, we reduce its contribution by a factor of $\sim$7 by a cut $|\cos\theta_{\gamma,\ \mathrm{beam}}| < 0.9$, see fig. 1b.

3.3 A_{ρ^*}

A_{ρ^*}=A$(\phi\to\rho^*\to\pi^+\pi^-\gamma)$, the γ being radiated from one of the pions. This process commonly called, *final state radiation*, contributes approximately one tenth of the *initial state radiation* background. However, $|A_{\rho^*}|^2$ is peaked at small values of $\theta_{\pi\gamma}$, see figure 6b of Ref. 2. We therefore restrict $|\cos\theta_{\pi\gamma}|$ to be less than 0.9, see fig. 1c. The sum of these three sources of background is shown in figure 1d, the solid line being without angular cuts, the dashed line with the two angular cuts of $|cos\theta|$ less than 0.9. With these cuts combined, we retain 80 % of the signal and improve the signal to background ratio, S/B, by a factor of 5–6, see figures 6 and 7.

3.4 $|A_{f_0}|^2$ AND $2\Re(A_{\rho^*}A^*_{f_0})$.

The angular dependence of $|A_{\rho^*}|^2$ is shown in figure 8a and 8b of Ref. 2. However the amplitude given in that reference ignores the bound quark pair wave function of the corresponding mesons, without which the amplitude blows up because of the k^3 factor characteristic of the emission of a photon of momentum k. We damp the amplitude following De Rújula, Georgi and Glashow,[7] with an exponential $Ae^{-x/\Gamma}$ where $x = s-(m_1+m_2)^2 = 2m_\phi E_\gamma$, Γ=300 MeV, and A=2.65 normalizes the damping factor to 1 at the f_0 peak (42.7 MeV). The signal size depends on the f_0 BR. We illustrate it for the two extremes for the range of interest, 1×10^{-6}, fig. 2a and 2.5×10^{-4} fig. 3a. We use 52% for BR($f_0\to\pi^+\pi^-$).[1]

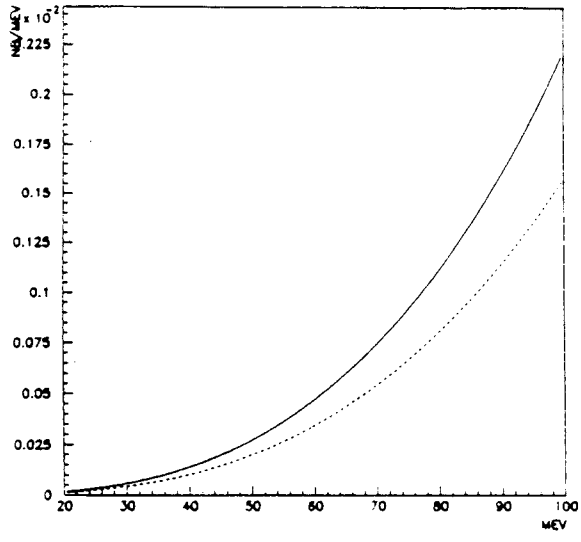

Fig. 1. a. $|A_1|^2$ contribution

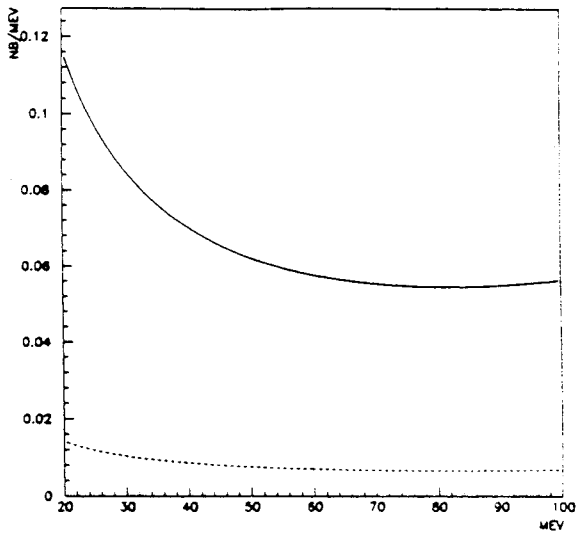

b. $|A_2|^2$ contribution

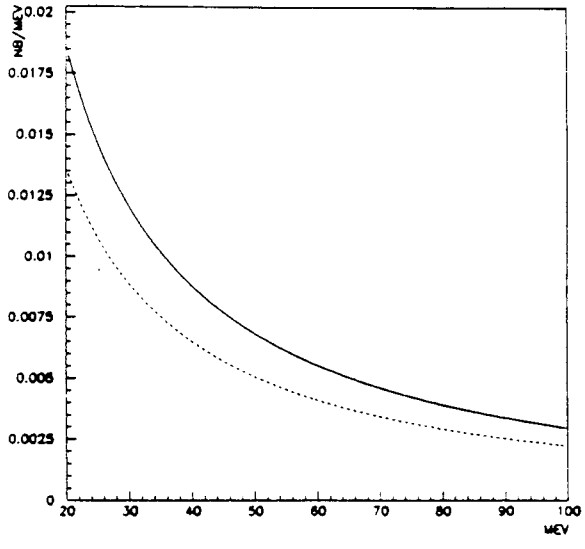

Fig. 1. c. $|A_{\rho^*}|^2$contribution

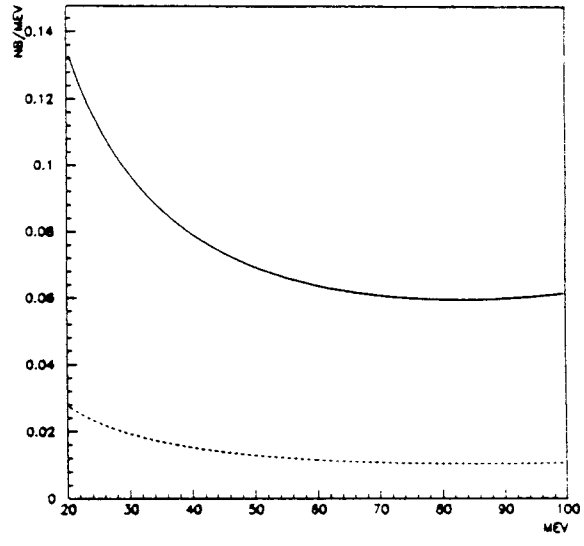

d. Total incoherent backgound

Solid lines are without angular cuts, dotted lines are for $|\cos\theta_{\gamma,\,\mathrm{beam}}| < 0.9$ and $|\cos\theta_{\pi\gamma}| < 0.9$, in all figures.

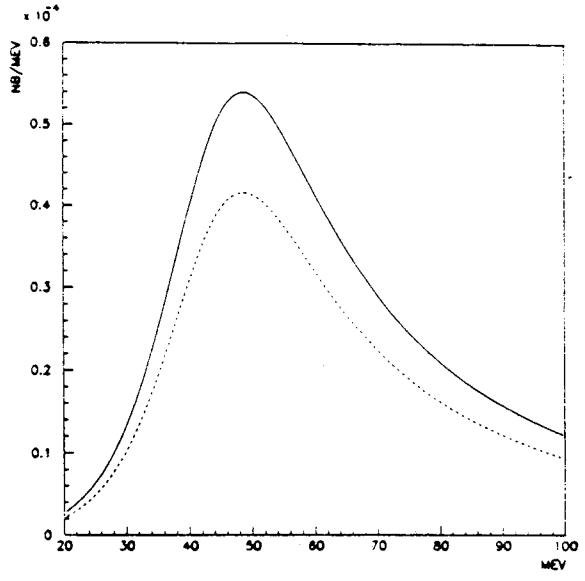

Fig. 2. a. γ spectrum: $f_0 \to \pi^+\pi^-\gamma$

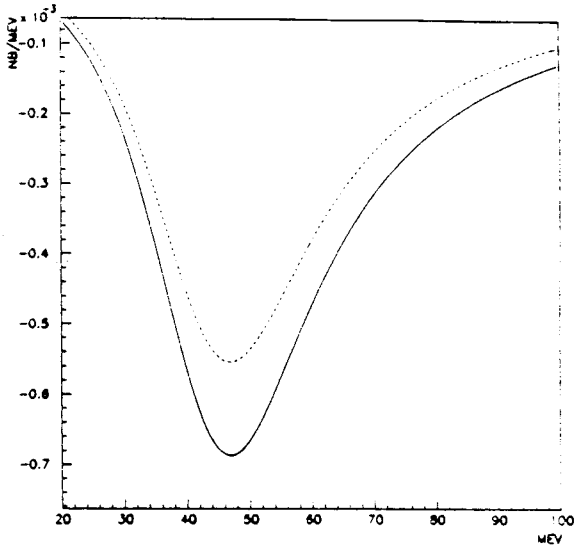

b. $2\Re(A_{\rho^\bullet} A^*_{f_0})$, BR=$1\times10^{-6}$

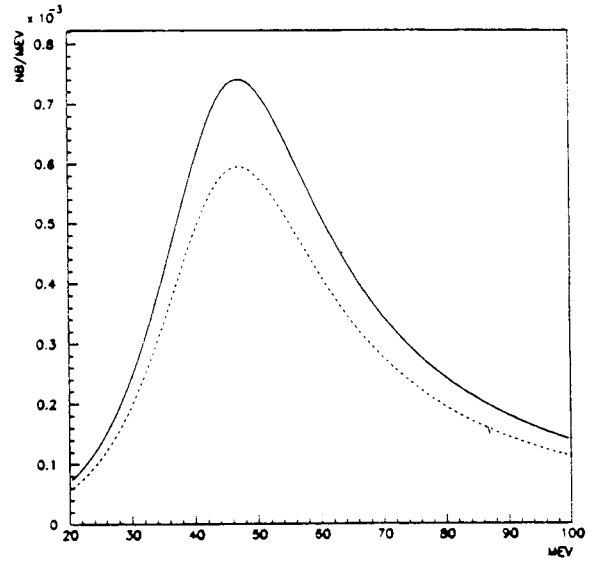

Fig. 2. c. $|A_{\rho^\bullet}|^2 - 2\Re(A_{\rho^\bullet} A^*_{f_0})$

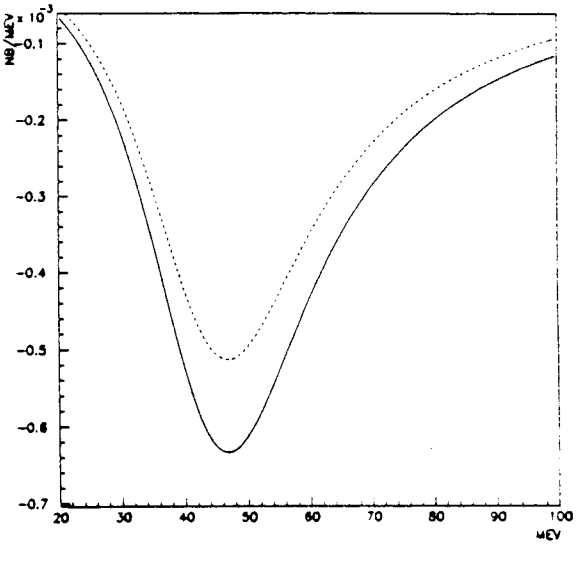

d. $|A_{\rho^\bullet}|^2 + 2\Re(A_{\rho^\bullet} A^*_{f_0})$, BR=$1\times10^{-6}$

Solid lines are without angular cuts, dotted lines are for $|\cos\theta_{\gamma,\,\mathrm{beam}}| < 0.9$ and $|\cos\theta_{\pi\gamma}| < 0.9$, in all figures.

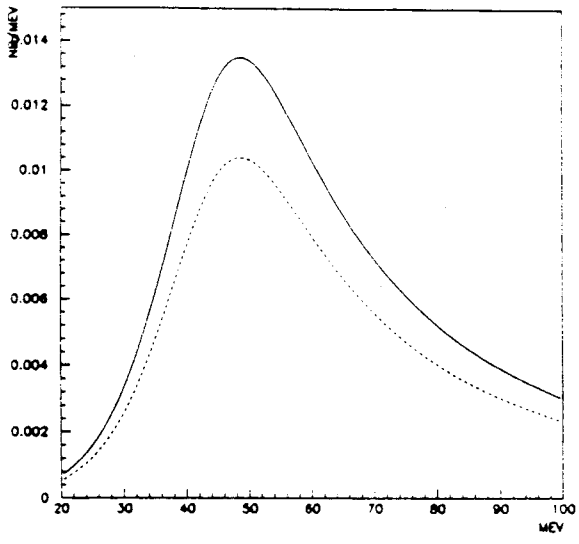

Fig. 3. a. γ spectrum: $f_0 \to \pi^+\pi^-\gamma$

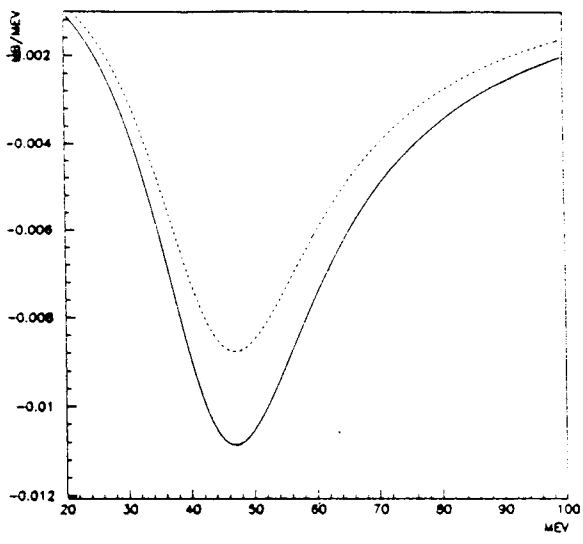

b. $2\Re(A_{\rho^0} A^*_{f_0})$, BR=$2.5\times10^{-4}$

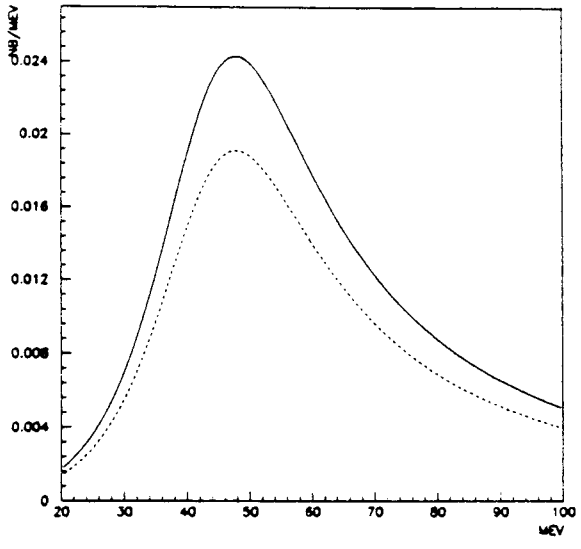

Fig. 3. c. $|A_{\rho^0}|^2 - 2\Re(A_{\rho^0} A^*_{f_0})$

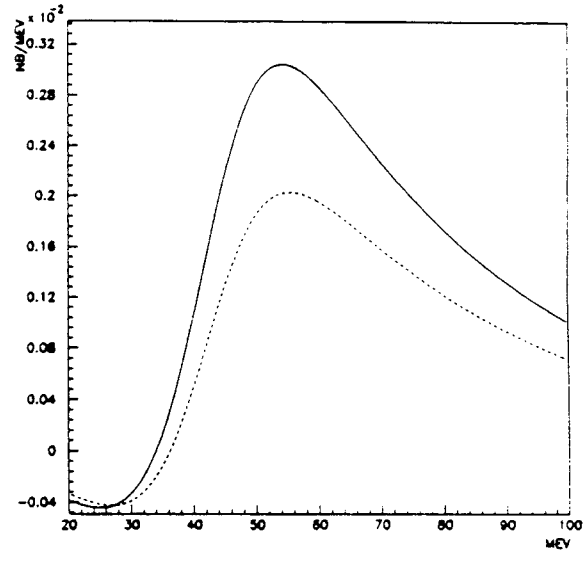

d. $|A_{\rho^0}|^2 + 2\Re(A_{\rho^0} A^*_{f_0})$, BR=$2.5\times10^{-4}$

Solid lines are without angular cuts, dotted lines are for $|\cos\theta_{\gamma,\,\mathrm{beam}}| < 0.9$ and $|\cos\theta_{\pi\gamma}| < 0.9$, in all figures.

As mentioned in section 1, $2\Re(A_{\rho^*}A^*_{f_0})$ can be positive or negative; we arbitrarily show it as negative in the figures. The angular dependence of the interference term is shown in figures 7a and 7b of Ref. 2. Its magnitude for BR= 1×10^{-6} is shown in fig. 2b, and for BR=2.5×10^{-4}, fig. 3b. Note that in the former case, in absolute value, it dominates over the f_0 term, while the reverse is true in the latter case. This interesting cross over is because $|A_{f_0}|^2$ is proportional to BR, whereas the interference term varies as $\sqrt{\text{BR}}$. For constructive interference, we always obtain a positive contribution to the total cross section, figs. 2c and 3c; while in the case of destructive interference, note that in the first case, fig. 2d, the signal subtracts from the total cross section, while in the latter case, fig. 3d, we have a positive contribution to the total cross section, albeit with an f_0 signal reduced by the interference term. For BR$\sim1.75\times10^{-4}$, the integrated contribution to the $\pi^+\pi^-\gamma$ cross section vanishes, however a dip appears at low γ energies and an enhancement at high γ energies, allowing detection of the f_0 signal.

The angular dependence of $|A_{f_0}|^2+2\Re(A_{\rho^*}A^*_{f_0})$ also depends on the relative strength of each term, of course reflecting that of the most dominant term. To illustrate the complexity of the situation, we chose BR=1.5×10^{-4}, where the two terms have about equal strength, and show $\mathrm{d}^2\sigma/\mathrm{d}E_\gamma\mathrm{d}\cos\theta_{\gamma,beam}$ vs E_γ, $\cos\theta_{\gamma,beam}$, and $\mathrm{d}^2\sigma/\mathrm{d}E_\gamma\mathrm{d}\cos\theta_{\pi\gamma}$ vs E_γ, $\cos\theta_{\pi\gamma}$ for constructive interference, in fig. 4a and 4b, respectively. The same quantities in the case of destructive interference are shown in fig. 5a and 5b respectively, where dips and enhancements are clearly visible. We also note that the relative strength of $|A_{f_0}|^2$ and $2\Re(A_{\rho^*}A^*_{f_0})$ are modulated by the γ–π angle, upon which A_{ρ^*} depends strongly.

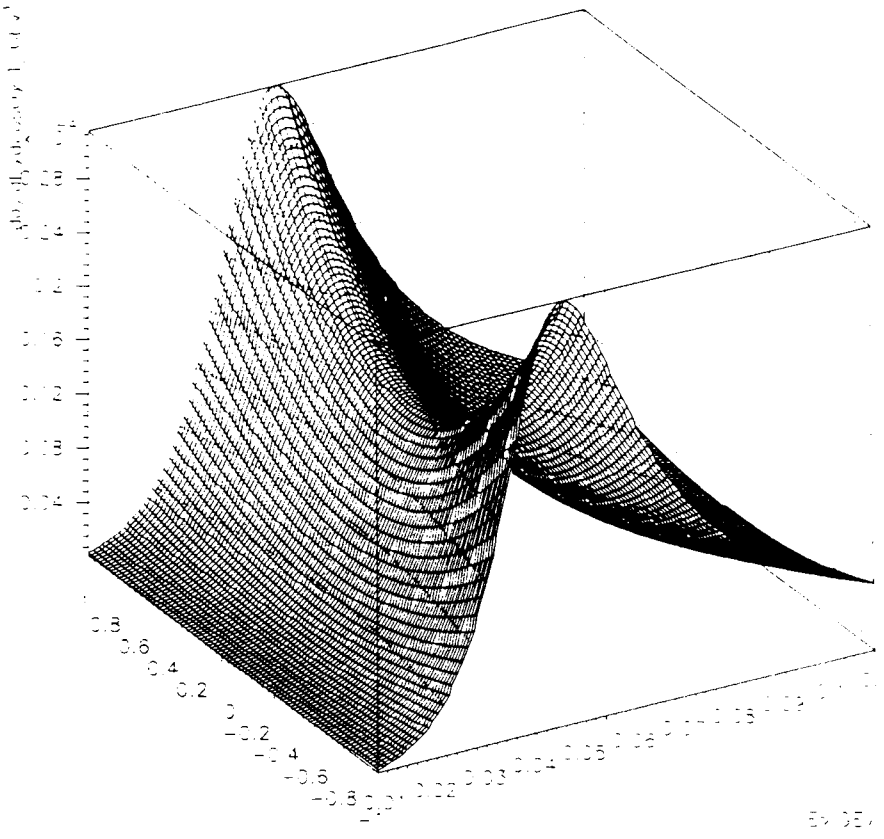

Fig. 4a. $d^2\sigma/dE_\gamma d\cos\theta_{\gamma,beam}$ *vs* E_γ, $\cos\theta_{\gamma,beam}$ for constructive interference, BR=1.5×10^{-4}

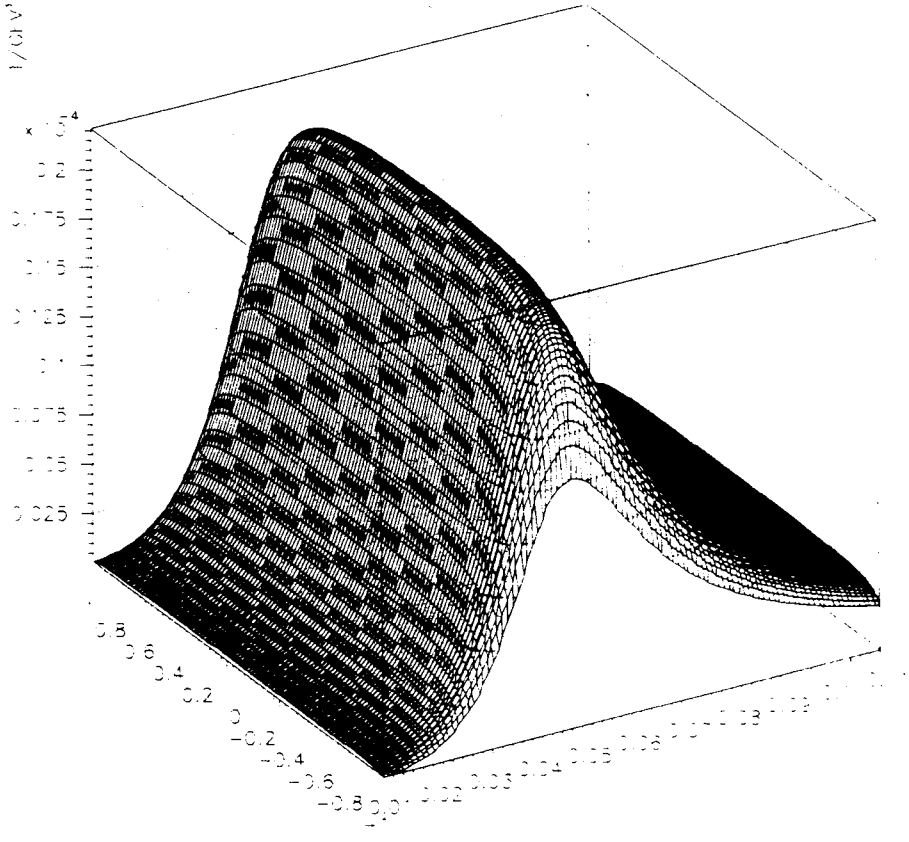

Fig. 4b. $d^2\sigma/dE_\gamma d\cos\theta_{\pi\gamma}$ *vs* E_γ, $\cos\theta_{\pi\gamma}$ for constructive interference, BR=1.5×10^{-4}

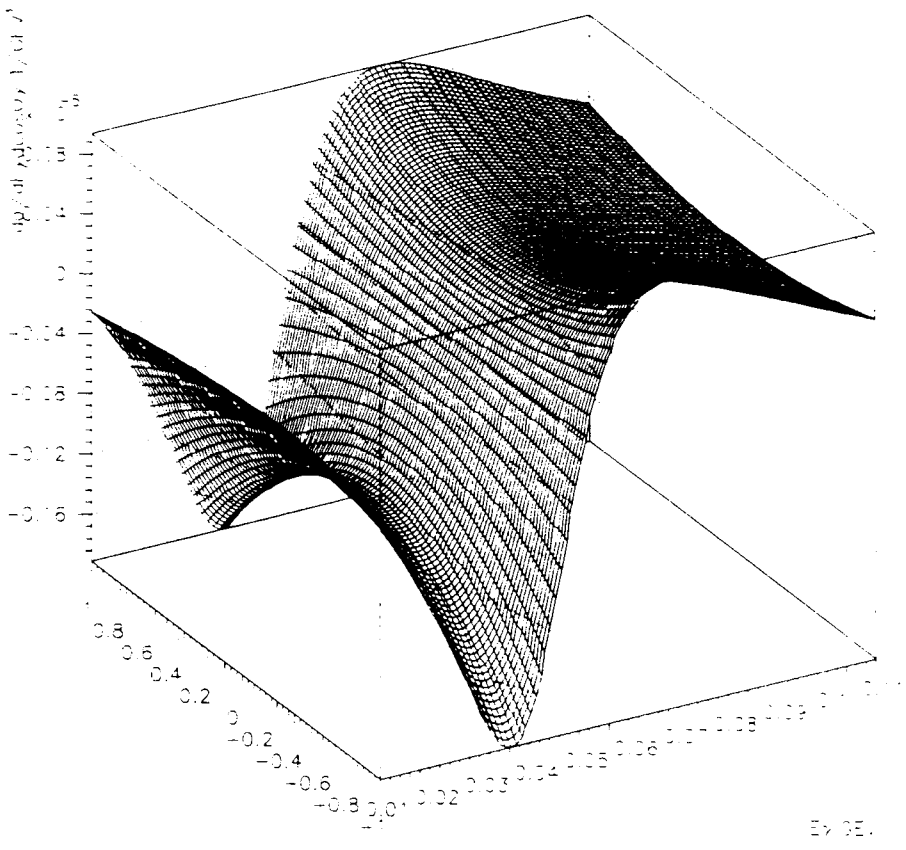

Fig. 5a. $d^2\sigma/dE_\gamma d\cos\theta_{\gamma,beam}$ *vs* E_γ, $\cos\theta_{\gamma,beam}$ for destructive interference, BR=1.5×10^{-4}

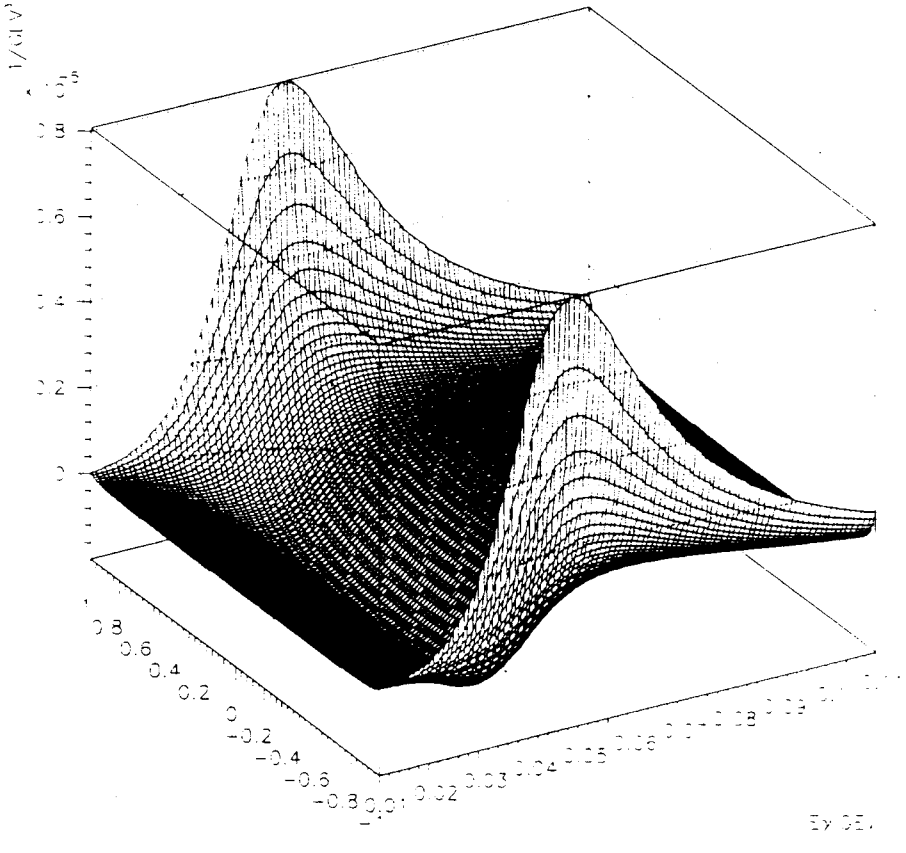

Fig. 5b. $d^2\sigma/dE_\gamma d\cos\theta_{\pi,\gamma}$ *vs* E_γ, $\cos\theta_{\pi,\gamma}$ for destructive interference, BR=1.5×10^{-4}

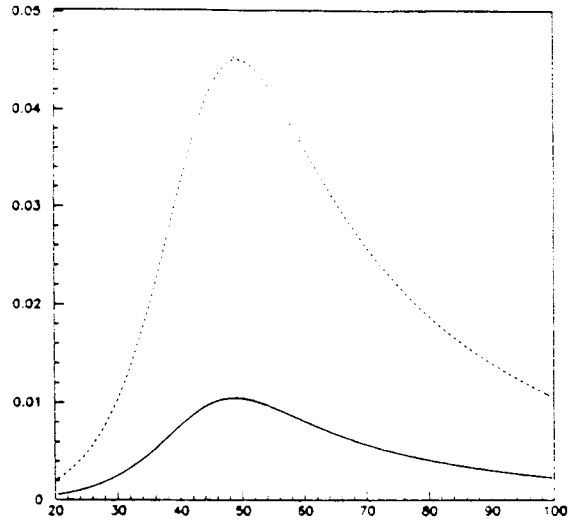

Fig. 6. a. S/B ratio for constructive interference, BR=1×10^{-6}

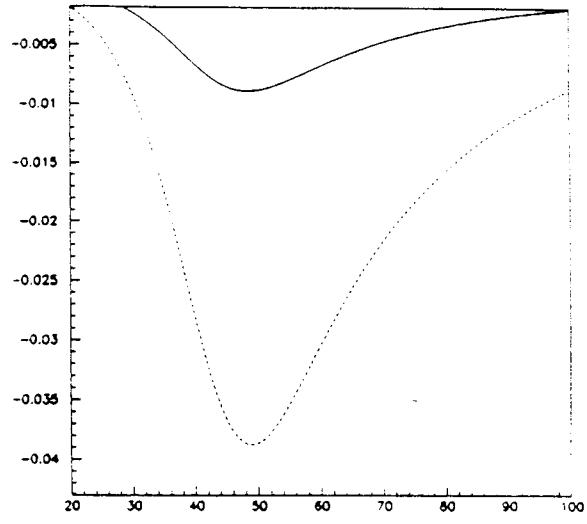

b. S/B ratio for destructive interference, BR=1×10^{-6}

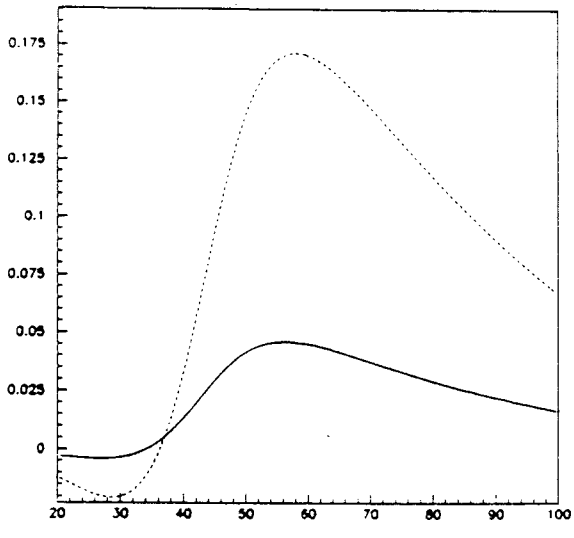

Fig. 7. a. S/B ratio for constructive interference, BR=2.5×10^{-4}

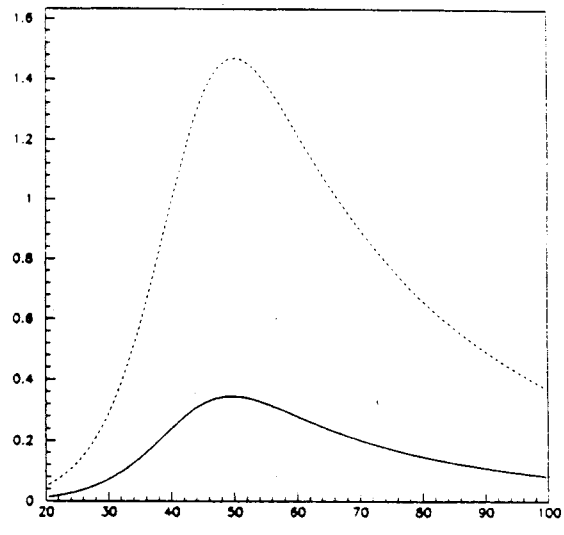

b. S/B ratio for destructive interference, BR=2.5×10^{-4}

Solid lines are without angular cuts, dotted lines are for $|\cos\theta_{\gamma,\ \mathrm{beam}}| < 0.9$ and $|\cos\theta_{\pi\gamma}| < 0.9$, in all figures.

4. Measuring the Signal

For BR=1×10^{-6}, the signal over the background cannot be shown directly. In order to demonstrate the effectiveness of the cuts we show the signal to background (S/B) ratio for the two cases of constructive and destructive interence, 6a and 6b. Note that in both cases we enhanced this ratio by about a factor of five, for a net effect of few %, for either destructive or constructive interference. With the expected DAΦNE luminosity the signal is quite measurable. Figure 7a, b show the S/B for BR=2.5×10^{-4}. The signal is certainly much larger and should be much easier to measure.

Figure 8 shows the MC simulated photon spectrum which would be observed in KLOE for $\phi\rightarrow f_0\gamma\rightarrow\pi^+\pi^-\gamma$ for the two cases, constructive and destructive interference, for BR=2.5×10^{-4} and assuming $5\times10^{+9}$ ϕ's are produced in the first year of DAΦNE's oprations. The incoherent backgound contribution is also shown, they are the solid, dashed and dotted histograms respectively.

We performed the *a priori* estimate calculation[8] to find the fractional accuracy that KLOE can achieve in one year's running at DAΦNE.

$$\frac{\delta(\mathrm{BR})}{\mathrm{BR}} = \frac{1}{\mathrm{BR}}\frac{1}{\sqrt{N}}\Big(\int\frac{1}{f(k)}\Big(\frac{\partial f(k;\mathrm{BR})}{\partial \mathrm{BR}}\Big)^2 \mathrm{d}k\Big)^{-\frac{1}{2}} \tag{4.1}$$

where

$$f(k) = \sum_1^3 \epsilon_{bcknd,i}\times \mathrm{BR}_{bcknd,i}\times g_i(k) + \epsilon_{signal}\times \mathrm{BR}_{signal}\times s(k).$$

The results are shown in figure 9, and give pleasant reassurance that even at the smallest BR considered and with destructive interference, the fractional accuracy is ten percent. In addition we note that the differential rate $\mathrm{d}^3\Gamma/\mathrm{d}E_\gamma \mathrm{d}\cos\theta_{\gamma,beam}\mathrm{d}\cos\theta_{\pi\gamma}$ clearly contains more information than the integrated cross section, thus it is possible to improve on the results presented. Finally, combining with measurements of $\phi\rightarrow f_0\gamma\rightarrow\pi^0\pi^0\gamma$ we can obtain a complete picture of the f_0.

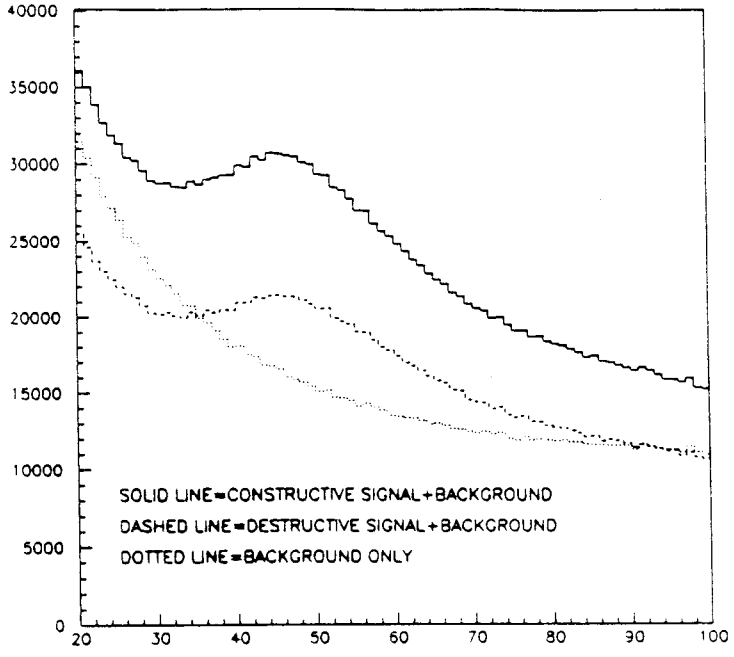

Fig. 8. Fig. 8. γ spectrum in KLOE from $\phi \to \pi^+\pi^-\gamma$ for BR=2.5×10^{-4} $5\times10^9\phi$'s

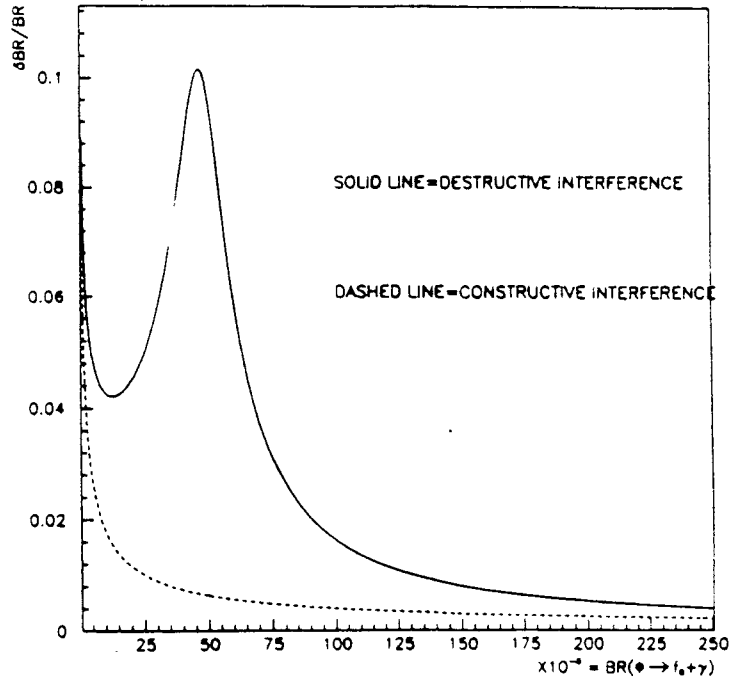

Fig. 9. Fractional error on BR *vs* BR

ACKNOWLEDGEMENTS

We wish to thank Paolo Franzini for discussions and help in preparing this paper.

REFERENCES

1. J. Lee- Franzini, Won Kim and Paula J. Franzini, these Proceedings, LNF Preprint 92/025 (P), April 1992.
2. A. Bramon, G. Colangelo, P. J. Franzini, and M. Greco, these Proceedings, LNF Preprint 92/022. April 1992.
3. N. Brown and F.E.Close, these Proceedings, RAL-91-085.
4. N.N. Achasov *et al.*, Phys. Lett. **96B**, 168 (1980).
5. KLOE Proposal, The KLOE Collaboration, LNF Preprint No. 92/019 (IR), April 92.
6. P. J. Franzini, G. Colangelo, LAPP Preprint ENSLAPP-A-379/92.
7. A. De Rújula, Howard Georgi, and S. L. Glashow, Phys. Rev. Lett. **37**, 398 (1976).
8. Paolo Franzini, these Proceedings, LNF Preprint 92/024 (P), April 1992.